

A Simulation of Gas Transport in Polymeric Membranes. Application to Heterogeneous Aging

J. Y. DOLVECK, P. DOLE, C. JOLY

Laboratoire d'Etudes des Matériaux Plastiques et des Biomatériaux, 43, boulevard du 11 novembre 1918, 69622 Villeurbanne Cedex, France

Received 13 August 1996; accepted 25 February 1997

ABSTRACT: A simplified mechanism of polymer aging has been proposed to simulate the effect of diffusion on degradation processes. Simple observations have been made on different events simulated using a modelization of the diffusion of low mass species: (1) the bulk oxidation rate, in the case of heterogeneous oxidation, is proportional to the square root of the initiation rate (formation of radicals). (2) The relative oxidation profile (relative to the surface oxidation) as a function of aging time is not constant. (3) The initial concentration of oxygen has, in some cases, a large influence on the apparent bulk oxidation rate during all the degradation processes. (4) The same observation is made for model samples stored in air and aged in inert atmosphere. (5) When heterogeneous oxidation occurs in samples containing antioxidant additives, the concentration of antioxidant has an effect on the induction period and on the bulk oxidation rate (this is not the case for homogeneous oxidation). (6) When heterogeneous oxidation occurs, the effect of antioxidant mobility can be practically neglected when $D_{\text{oxygen}}/D_{\text{antioxidant}}$ (D = diffusion coefficient) varies from 100 to 1. (7) The time required to reach a pseudostationary state (corresponding to the equality of oxidation rate and oxygen diffusion rate) can be interpreted by a simple induction period (antioxidant consumption and/or hydroperoxide accumulation). © 1997 John Wiley & Sons, Inc. *J Appl Polym Sci* **66**: 435–444, 1997

Key words: stimulation; heterogeneous aging; oxidation profile; crosslinking; diffusion properties

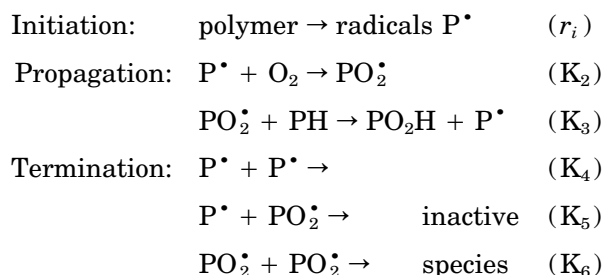
INTRODUCTION

Most polymer aging mechanisms involving oxidation phenomena lead to problems of heterogeneous degradation when thick samples are involved.

Literature has first focused on the problems of characterization of oxidation profiles by infrared microscopy¹ and indirect methods.^{2,3}

The second interest in this research area is the modelization of oxidation profiles.^{4–6} A general

model is currently accepted concerning the case of polyolefins.⁶



Assuming that a stationary state is obtained, the rate of oxygen consumption can be written as follows:

Correspondence to: P. Dole.

Journal of Applied Polymer Science, Vol. 66, 435–444 (1997)
© 1997 John Wiley & Sons, Inc. CCC 0021-8995/97/030435-10

$$r_{[O_2]} = \frac{\alpha[O_2]}{1 + \beta[O_2]}$$

For high oxygen concentration, $r_{[O_2]} = \alpha/\beta$, and for low values of oxygen concentration, $r_{[O_2]} = \alpha[O_2]$.

A transition domain is observed for $[O_2]_c \approx \beta^{-1}$.

When heterogeneous degradation is obtained, it can be considered that a stationary state is reached between the oxygen diffusion process (assuming Fick's law) and oxygen consumption:

$$D = \frac{\partial^2[O_2]}{\partial x^2} - r[O_2] = 0.$$

When $[O_2] < [O_2]_c$, the relative oxidation (relative to the surface) at a distance x from the surface is equal to:

$$R(x) = \frac{\cosh(\sqrt{k/D}(k - L/2))}{\cosh(\sqrt{k/DL/2})}$$

where k is the first order constant rate.

When

$$[O_2] > [O_2]_c, R(x) = 1, \quad r_{[O_2]} = cste = r_0,$$

$$\text{and } [O_2] = [O_2]_s + (r_0/2D)x(x - L)$$

where $[O_2]_s$ is the oxygen concentration at the surface.

The third interest is to understand the effect of heterogeneous degradation on the bulk properties of macromolecular materials. In some cases the evidence of heterogeneous degradation is made directly by complete changes in properties: for example, increases of tensile strength at high γ dose rate or high temperature (crosslinking reactions), and decrease of tensile strength at low temperature or low γ dose rates (chain scission reactions).^{7,8} In other cases heterogeneous oxidation has only an incidence on the bulk apparent rate of bulk property changes⁹: the more heterogeneous is the oxidation, the less is the apparent degradation rate. This leads to an apparent variation of the activation energy.¹⁰ Finally, in other cases mechanical properties are connected to the degradation of the material at the surface, but not connected to the whole degradation of the material.¹¹ Some more complex effects of the diffusion limited processes have never been treated: effect of the initial oxygen concentration, effect of anti-

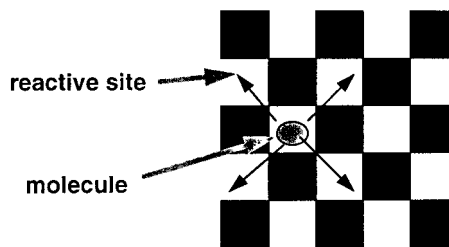


Figure 1 Molecule displacements.

oxidant diffusion rate, induction time connected to the reach a stationary state. These points will be discussed in this article, which proposes a simple simulation method of degradation processes in polymers. The advantage of such a model is to observe simultaneously the evolution of the concentration profile of the different species, and the variation of chain scission and crosslinking events within the bulk.

Simulation

Diffusion

The diffusion model derives from a geodesic concept. The polymeric membrane section is represented as a regular network of pixels that are the "nets." The displacements of the diffusant molecules follow definite lines between two nets (Fig. 1). To give an idea of the dimensions simulated, the separating length between two nets is considered to be about 0.5 nm. All the elementary displacements have, therefore, the same length. In this case, the chosen network is a two-dimensional square angle lattice, in order to construct a simple computer image. For esthetic reasons the sites are disposed as on a draughtboard. The displacements are then oriented in the diagonal directions according to Figure 4, but the directions are random, using the random function of the computer. The two faces of the membrane are represented by vertical lines. The thickness of the membrane is then given by the number of nets between these limiting lines. In the given results, the membrane is 100 pixels high. According to the choice of the draughtboard shape, only half of the sites are limiting the membrane on each side. The considered thicknesses vary from 10 to 100. For the maximum thickness, the number of accessible sites in the whole membrane is then 5000.

The algorithm runs in loops, during which time all the molecules present in the membrane are displaced. The duration of a loop is the unity of

time. At the beginning of each cycle a defined number of new molecules are implanted on both limiting lines. The unity of pressure is then the number of the incident molecules per limiting site. The number of impacts is defined but the localization of an impact is random. The condition of adsorption is that the chosen limiting sites must be empty. Thus, the displacements for all the molecules are random and at least the molecules will be moved one after another according to the initially chosen displacements. It takes into account the fact that two molecules cannot occupy the same position. A given molecule is displaced after a test of vacancy of the receiving site: if the site is yet occupied, the orientations of the displacements of the incident and the placed molecule are inverted. Here, the test of vacancy consists arbitrarily in three consecutive attempts. Then, if no solution is found to place the incident molecule, this will be stopped. The reality of our method of arbitration will not be discussed in this article.

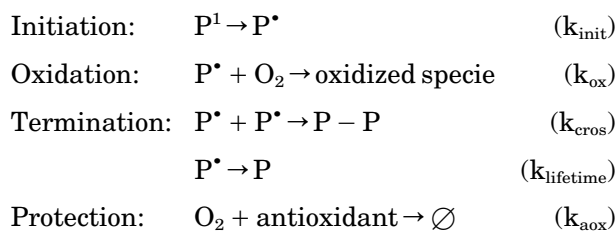
The desorption event occurs when a diffusing molecule crosses one of the limits. This can, therefore, occur at any moment of the sequence of the displacements of the molecules.

In this simulation where the membrane has only two dimensions, assuming the fact that the frequency of jumps is equal to 1 in this case and that the displacements are diagonal, the value of D in the ideal case will be equal to:

$$D = \frac{1}{4} * 1,414^2 = 0,5 \text{ in pixel unities.}$$

Reactions

To simplify the modeling of the degradation process, the mechanism described above has been reduced:



Reaction rates are proportional to the number of sites taken randomly (among all types of polymer sites) per loop in the program.

Reactions between two species are possible if the first one is chosen among the sites taken randomly and if the second species is adjacent to the first one.

The modeling of the five types of reactions is not made with a given order for each loop. All reactions, whatever their type, are considered in a random order.

The consideration of the reaction of oxygen with the antioxidant additive is approached differently. k_{aox} is supposed to have an infinite value. The reaction is concomitant with the modeling of the displacement of molecules. Before the displacement of oxygen and antioxidant additive, adjacent pairs of oxygen/antioxidant are destroyed.

Two different methods could be chosen to model the displacement of antioxidant additive, which has necessary a lower diffusion coefficient compared to the diffusion coefficient of oxygen (a times minor): make the displacement of 1/a molecules at each loop, or make the displacement of all molecules every "a" loops. The second method has been chosen.

The mechanism proposed here does not correspond to the reality (no propagation with the hydroperoxy radical). But the kinetics of oxygen consumption should be the same: for low concentrations of oxygen, first-order kinetics, and zero-order kinetics for high partial pressure of oxygen, because when a critical oxygen concentration is reached, all activated sites (radical) present at least one oxygen molecule on adjacent sites.

Parameters

Thickness: to obtain heterogeneous degradation, high thicknesses of 100 pixels are mainly considered in this study. However, in the first part, where unperturbed oxidation kinetics are studied, homogeneous behavior is necessary. In contrast, a value of only 10 pixels has been taken for this particular case.

Oxygen pressure: with the exception of the study of oxidation kinetics and the study of the effect of oxygen concentration, high values of oxygen pressure will be preferred to observe zero-order and first-order kinetics regions on the thick sample.

Antioxidant partial pressure has been taken as equal to zero. This case corresponds generally to real aging conditions except for aging in an enclosed atmosphere.

Constant rates are expressed by the probability of reaction of each site per loop of the program.

Oxidation of crosslinked sites: taking into account steric perturbation of these events the constant rate of the reaction has been taken as equal to zero.

Oxygen initial concentration has been gener-

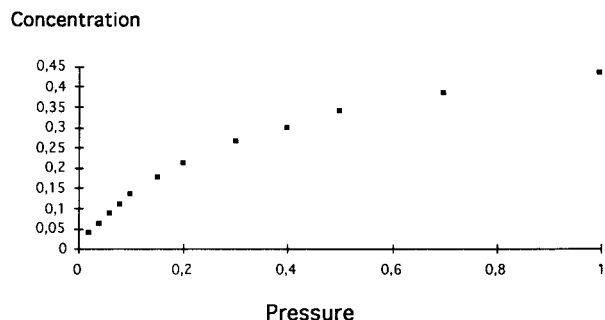


Figure 2 Isotherm of sorption of the simulated sample.

ally taken equal to zero. This case does not correspond to the real aging conditions or the accelerated aging conditions. The problem of the initial concentration is that the initial conditions are often unknown (equilibrium of sorption or not, and difference of solubilities between storage and accelerated aging conditions).

Antioxidant concentration: except for the study of the effect of antioxidant additive, this value has been taken equal to zero (pure mechanism).

Crosslinking constant rate: same remark as above.

Oxidation constant rate: as in real cases, this constant has generally been taken as quite high: 0.1, 0.5 (control of the kinetics principally by the initiation process).

Initiation constant rate: taking into account the last remark, this value has been taken quite low: generally 0.004.

When no crosslinking events are modeled, it is important to impose a termination event in order to limit the accumulation of radicals. The lifetime of radicals has been taken as equal to 100 loops.

RESULTS AND DISCUSSION

Characterization of the System

The sorption isotherm is given in Figure 2. As two molecules cannot occupy the same site, Henry's law is verified only for low concentrations. The shape of the isotherm corresponds, in fact, to a Langmuir equation. Authors want to underline that the simulation suppositions do not correspond to a Langmuir type sorption because molecules are not adsorbed on Langmuir sites. The interest of this "false" Langmuir simulation will be exposed in another publication. In this article, only the effect of oxygen concentration will be discussed.

Using the isotherm, given values of oxygen concentration can be imposed by control of oxygen pressure. The variation of the number of oxidized sites has been recorded at each imposed oxygen concentration (thin membrane, 10 pixels thick, in order to obtain homogeneous degradation process). Assuming that the kinetics of oxidation is first order, first-order constants can be calculated taking the slope of $\ln(1 - X) = f(t)$ curves (X = conversion yield). The usually observed variation of the first-order constant rate of oxidation is verified in our simulation. The basic scheme generally proposed is found again: first-order kinetics at low oxygen concentration and zero-order kinetics at high oxygen concentration. For $k_{ox} = 0.5$, the critical oxygen concentration is closed to 0.06. This value varies with k_{ox} : when k_{ox} decreases, the critical oxygen concentration increases (cf. Fig. 3).

Effect of Initiation Rate

The effect of initiation rate on oxidation profiles is often modeled by the simple method of the TOL = thickness of oxidized layer.^{12,13} The TOL is defined as the half thickness of a sample that reaches the critical oxygen concentration in the middle of the cross section. This method is also applied to the case of zero-order kinetics:

$$\begin{aligned}
 [O_2]_{x=1/2} &= [O_2]_c = [O_2]_s + \frac{r_o}{2D} \times (x - L) \\
 &= [O_2]_s - \frac{r_o(2TOL)^2}{8D} \\
 TOL &= \sqrt{\frac{2D([O_2]_s - [O_2]_c)}{r_o}}.
 \end{aligned}$$

In the case of γ irradiation, it can be assumed that the initiation rate is proportional to the dose rate.

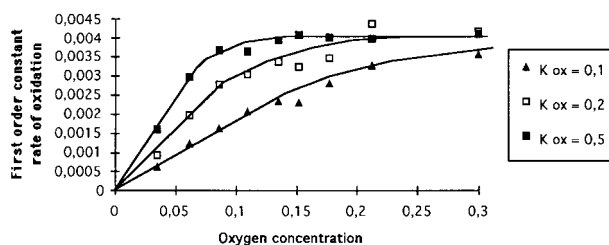


Figure 3 Effect of the oxidation constant rate on the critical oxygen concentration.

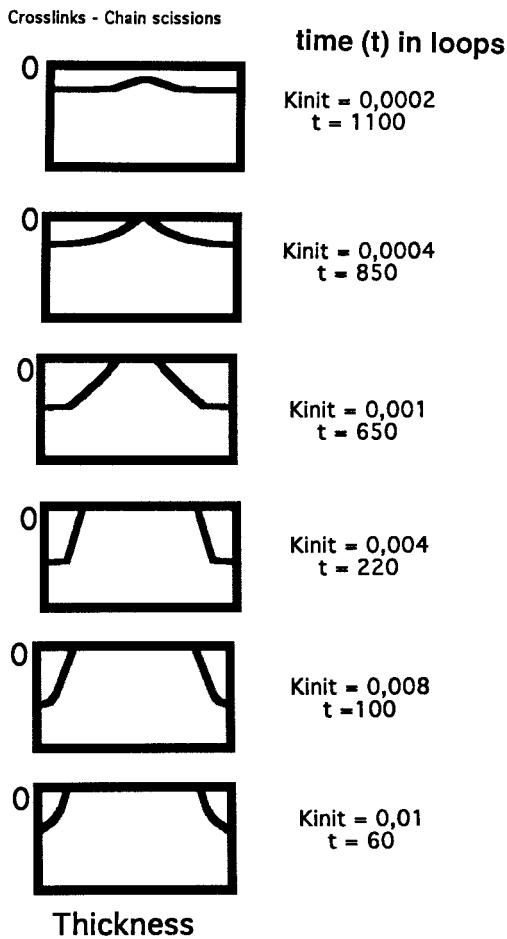


Figure 4 Effect of the initiation constant rate in the case of heterogeneous oxidation profiles.

Considering the mechanism described in the introduction, the unperturbed oxidation rate r_o should also be proportional to the square root of the dose rate. Also, the thickness of the oxidized layer should be proportional to the reciprocal of the square root of the square root of the dose rate. However, Papet¹² showed in the case of the simplest polyolefin (although polyethylene should follow perfectly the model generally given in the bibliography) that the thickness of the oxidized layer was proportional to the reciprocal of the square root of the dose rate.

In the case simulated in this study, the simplified mechanism proposed leads to a proportionality between k_{init} and the first-order constant rate of oxidation: it can be verified that the limit values of the first-order constant rate of oxidation are equal to the k_{init} imposed values when these observations are made in the case of thin membranes (10 pixels). With thick simulated samples (100

pixels), heterogeneous oxidation is observed. Oxidation profiles, presented in Figure 4, are shown as mass profiles: each oxidation event is assumed to induce a chain scission, and is also counted negatively. It can be seen in Figure 4 that a negative variation of TOL with this dose rate is observed, as predicted by the equation given above. But it can be observed that the measurement of the TOL would be quite difficult in this case.

The bulk variation of the oxidation yield in the case of heterogeneous oxidation profiles has been studied. It can be observed in Figure 5 that when the evolution is shown as a function of a reduced time scale (aging time multiplied by initiation constant rate) no master curve is observed. This phenomena is observed in the case of real aging mechanisms. Particularly, the reduced time should represent a γ dose. For a given dose, the authors have often observed a decrease of the degradation yield with increasing dose rate. This problem is directly due to the heterogeneity of the sample. Even if heterogeneous degradation occurs, an apparent (average value) first-order constant rate of oxidation can be calculated (a nearly linear relation of $\ln [(1 - x) = f(\text{time})]$).

The variation of this constant with the square root of the initiation constant rate is shown in Figure 6. A linear variation is obtained. It must also be underlined that if a linear dependence with the square root of the initiation rate is obtained, the method is not the same as the method of TOL. The method of the total integral used here (bulk variation of oxidation yield) takes into account the two different regions of the oxidation profile: zero-order kinetics region at the surface and first-order kinetics region in the bulk. In the

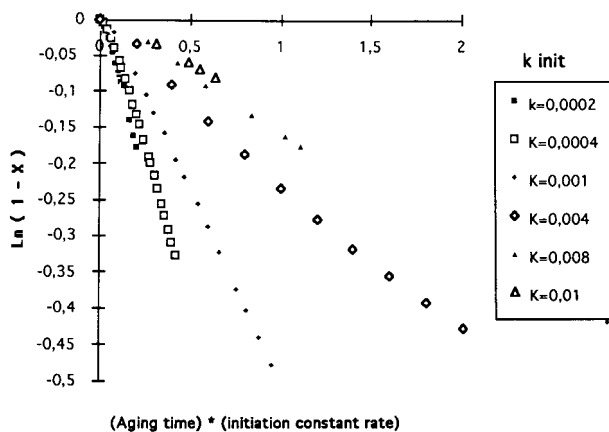


Figure 5 Effect of the initiation constant rate: simulation of a dose effect.

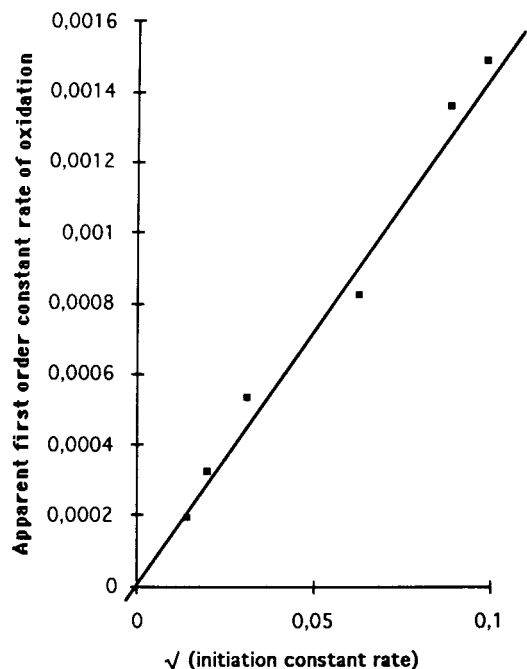


Figure 6 Variation of the apparent first-order rate of oxidation as a function of the square root of the initiation constant rate.

case of TOL, only the first one is considered. In fact, as the zero-order oxidation rate and the first-order constant rate are both proportional to r_i (in the simulated mechanism) a similar variation with r_i is observed.

Effect of Oxygen Initial Concentration

Degradation mechanism studies are often made on thin films of pure polymers, because most of these studies are made by FTIR analysis, which require such samples. In this case, it can be assumed that oxygen solubility is reached quite quickly. But when mechanical properties or other physicochemical properties are studied, thick materials are often used. Pauly¹⁴ made the calculation of oxygen profiles of 4 mm-thick unsaturated polyester samples, which were destined to be aged by γ irradiation: solubility is reached after 100 days of storage time at ambient temperature. In the case of a phenolic plastic, solubility is reached after 100 years of storage.

Even if samples are stored for a sufficient time, another problem must be considered concerning thermal aging: when samples are put in ventilated ovens for accelerated aging, they are submitted to a temperature variation from 20 to 100°C or more. Oxygen solubility varies drastically. The

decrease can be considerable (solubility divided, for example, by 2 when the variation is 100°C). Under these conditions, the aging mechanism is not representative. The two situations above have been simulated and compared to a situation without oxygen at time 0. At the chosen pressure (0.2) the equilibrium concentration is equal to 0.2. It can be seen in Figure 7 that the three situations are very different: (a) first case: oxygen initial concentration = 0. The oxygen profile becomes constant almost instantaneously; stationary state between oxygen diffusion and oxygen consumption is reached. (b) Second case: oxygen initial concentration = oxygen solubility. The oxygen profile varies slowly from the strength line to the constant profile of the previous case. The oxidation is homogeneous during this first step. (c) Third case: oxygen initial concentration = oxygen solubility $\times 2$.

In the first step a desorption profile is observed. The second step corresponds to the previous case. As the equilibrium concentration is greater than the critical oxygen concentration, no incidence of the desorption step is observed on the oxidation profile. However, the period of homogeneous oxidation increases.

Figure 8 shows the evolution of the bulk oxidation yield with aging time in the three conditions described. The excess of oxygen ("excess" compared to the stationary oxygen profile) leads to the observation of an apparent induction period, which could be interpreted in a chemical mechanistic way if the degradation was considered to be homogeneous: accumulation of a reactive species, change of mechanism, etc. Moreover, the slope of the curves in their second step is different. The oxidation rate appears to be higher in the case of simulated samples with high oxygen concentration. This is only due to the fact that oxidation profiles are different, and also that the apparent bulk oxidation rate is different (the bulk rate has to be distinguished from the local oxidation rate).

This remark should be better illustrated at a high oxygen pressure in our simulation algorithm, such as $P = 0.8$. Thus, the initial concentrations used above are less than the solubility. No apparent induction period is observed; the oxidation profile is different in the three cases, and also, as in the previous cases, the apparent bulk oxidation rate increases with the initial oxygen concentration (even if the initial oxygen quantity is quickly consumed).

Aging in Inert Atmosphere

If the outside oxygen pressure is equal to zero, the simulation can be compared to aging in inert

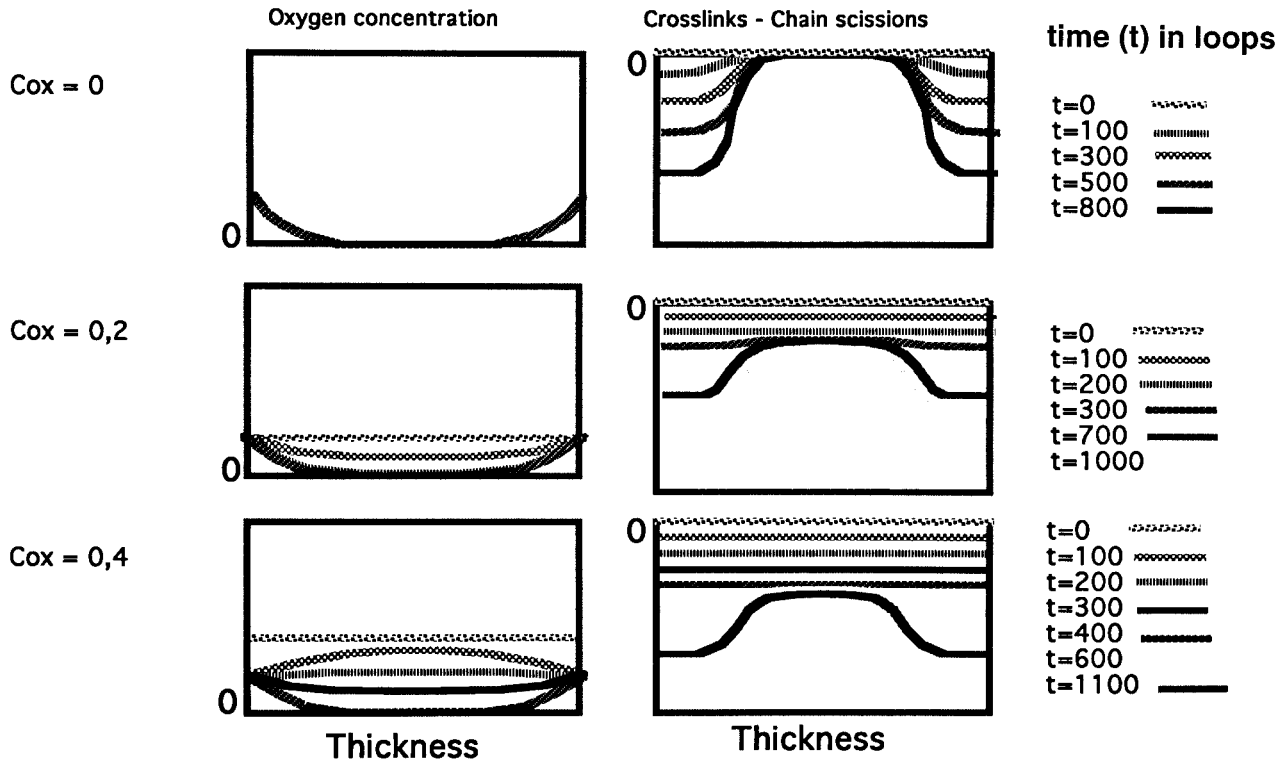


Figure 7 Effect of oxygen initial concentration for samples under low pressure profiles.

atmosphere. The first-order kinetic is followed in the first step of the process (excess of oxygen). It is obvious that when the oxygen initial concentration increases, the maximal oxidation yield also increases. The interesting result is that in this case the oxidation profile, which would be inverted. The sample is more degraded in the bulk than at the surface, which corresponds to the

shape of the desorption profile. It could be evidenced that at short time, aging in an inert atmosphere is similar to an aging at the pressure, which corresponds to the initial concentration. Such types of aging should be interpreted as post-annealing, postvulcanization in real cases and not oxidation. It must be emphasized that in these cases, the oxidation yield at the surface is equal to zero, and this can lead to mistakes in interpretation if only surface analyses are made.

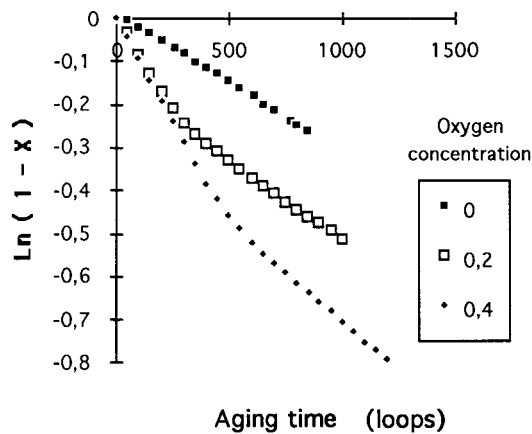


Figure 8 Effect of oxygen initial concentration for samples under low pressure kinetics.

Aging of Protected Samples

Contrary to homogeneous aging, Figure 9 shows that when heterogeneous degradation occurs, no important induction time is observed, the consumption of antioxidant occurs progressively throughout the degradation process, and is directly connected to the variation of oxygen and antioxidant profiles. Oxygen diffuses progressively in the bulk and the antioxidant profile also decreases progressively. Another consequence of this phenomena is that the apparent first-order constant of oxidation varies with the antioxidant concentration. Verdu¹⁵ showed the same type of

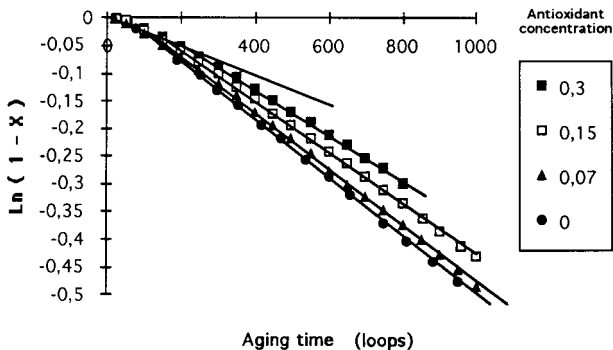


Figure 9 Effect of antioxidant concentration kinetics.

profiles in the case of “real” samples of crosslinked polyethylene.

The effect of the diffusion coefficient has been studied in the range

$$1 < \frac{D_{O_2}}{D_{Antiox}} < 100.$$

A small effect can be observed on the profiles in Figure 10. The greater the antioxidant mobility is, the better the protective effect of the additive is. Two points must be stressed. In fact, it can be verified that very weak effect on the evolution of the bulk oxidation yield is observed. This observation should not be made in the case of homogeneous oxidation (lower oxidation constant rate value, and lower antioxidant consumption rate value). In this case, the desorption profile of antioxidant additive should be observed, and as a consequence, the antioxidant efficiency should be lower for high values of antioxidant mobility.

Crosslinking/Chain Scissions

The evaluation of the aging of materials is often made by mechanical properties. The end-life criteria employed is often the half value of the initial ultimate elongation. In the case of γ irradiation of polymeric materials, Wilsky showed that this value was corresponding to a constant lethal dose for low dose rates (homogeneous oxidation) and was increasing with increasing high dose rate (heterogeneous oxidation) up to a constant value in some cases (equivalent to aging in inert gas).^{16,17} In some cases, this evolution is only due to the decrease of oxidation reaction in the bulk at high dose rates. In other cases, this evolution is also due to the occurrence of crosslinking reactions in the bulk. Clough and Gillen showed by

modulus profiling the different cases of degradation profiles that could be obtained.¹⁸ Consider the effect on the whole properties evolution: in the proposed simulation, it has been considered that all oxidation events led to a scission reaction; moreover, this event occurs instantaneously. This, of course, does not reflect the reality. The results are presented using the difference of the numbers of crosslinking events and chain scission events (N).

When crosslinking constant rate is significant compared to the oxidation, it has been verified that the bulk evolution can be, in fact, considered as a pure crosslinking modification, although the modifications at the surface correspond to a pure oxidative mechanism.

When the oxidation constant rate is more significant, two interesting situations can be observed (Fig. 11): (1) N reaches a maximum value and then decreases: the decrease is due to the stable oxygen concentration profile being reached, or (as the case here) the decrease is due to the high consumption of reactive sites in the bulk during the first step of the process (second order reaction of crosslinking). (2) When K crosslinking is very low, no increase of N is observed. The first case described should be interpreted by postcuring effects on unaged material, and the second case should be interpreted as an induction period.

c antiox = 0,3

t=500 loops

Dox/Dantiox = 100
Dox/Dantiox = 1

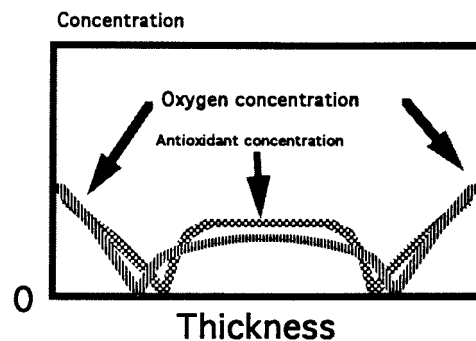


Figure 10 Effect of antioxidant mobility profiles.

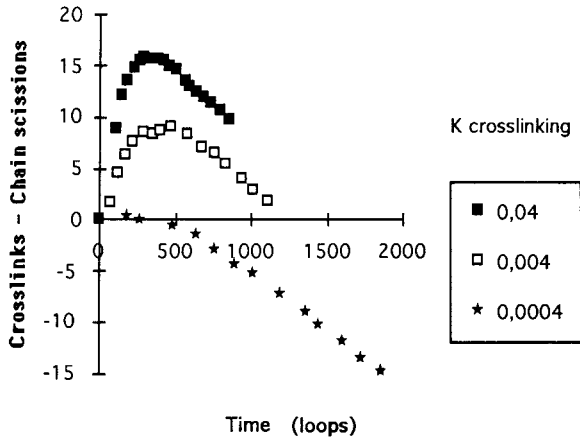


Figure 11 $k_{ox}/k_{cross} = 1$; effect of crosslinking constant rate kinetics.

Pseudoconstant Oxidation Profile

The last point that must be underlined is that some articles often present the results of microdetermination of heterogeneous oxidation with relative oxidation profiles. Contrary to the general understanding, as the oxidation kinetics are first order (relative to reactive sites), the oxidation profile is not constant, as shown in Figure 12.

CONCLUSION

Simulations of heterogeneous degradation may constitute a new approach to the study of polymer

aging. The model presented in this article is calculated with a simplified mechanism that only leads to general remarks on heterogeneous degradation: (1) the square root of the initiation constant rate is proportional to the bulk oxidation rate, when total heterogeneous oxidation occurs (no oxidation in the bulk material). (2) The initial concentration of oxygen has a large incidence on the evolution of the bulk oxidation yield in all cases simulated: aging in inert gas, aging in conditions where the oxygen solubility is less or more than the solubility in initial storage conditions. (3) Antioxidant concentrations can influence the apparent oxidation rate in heterogeneous degradation conditions, even if the oxidation is totally inhibited in homogeneous degradation conditions (the so-called induction period of antioxidant consumption). (4) When crosslinking reactions occur in the bulk material, different types of evolution can be observed, easily leading to errors in interpretation. (5) It has been clearly illustrated that oxidation profiles are not constant with aging time.

The second part of this study is presently being studied: simulation of a complex oxidation mechanism taking into account all types of radical secondary reactions leading to chains scissions, accumulation of hydroperoxides, and all possible types of termination reactions. The spatial repartition of all types of species should open new fields of

$P_{ox} = 0,3$
 $K_{init} = 0,001$
 $K_{ox} = 0,5$

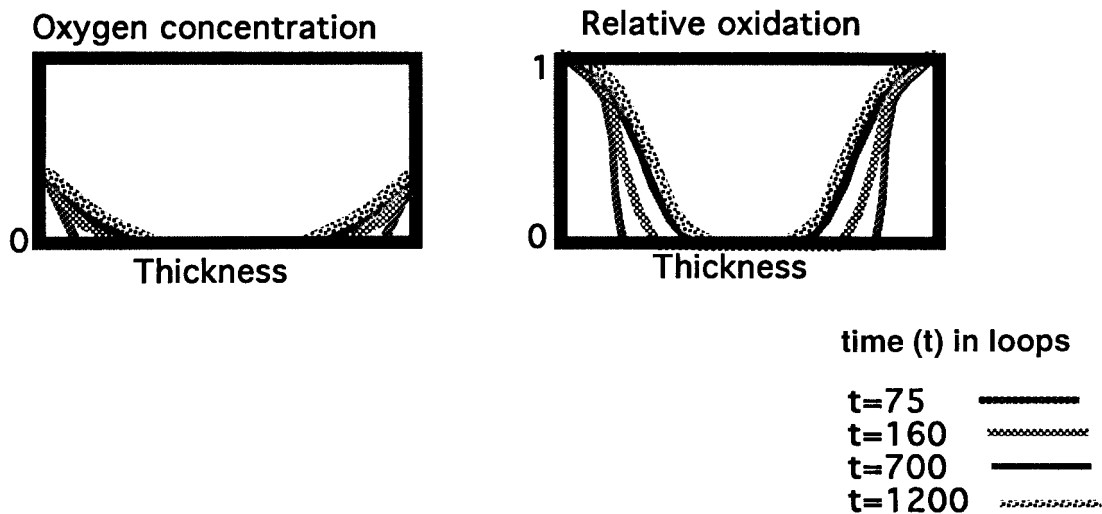


Figure 12 Variation of the relative oxidation profile.

investigation. Another interesting field of research should be the simulation of the degradation of a semicrystalline polymer, which exhibits different types of degradation areas, having different behavior concerning oxygen diffusivity: amorphous and crystalline phases and tie molecules regions, which have a determining effect on the mechanical properties of polymers.

REFERENCES

1. J. Lemaire, J. L. Gardette, and J. Lacoste, *Makromol. Chem., Macromol. Symp.*, **70/71** 419 (1993).
2. R. L. Clough and K. T. Gillen, *Polym. Degrad. Stabil.*, **38**, 47 (1992).
3. P. Dole and J. Chauchard, *Polym. Degrad. Stabil., Macromol. Chem. Phys.*, **195**, 3949 (1994).
4. K. M. B. Jansen, *Polym. Eng. Sci.*, **34**, 1619 (1994).
5. K. T. Gillen and R. L. Clough, *Polymer*, **33**, 4358 (1992).
6. L. Audouin, V. Langlois, and J. Verdu, *J. Mater. Sci.*, **29**, 569 (1994).
7. K. T. Gillen and R. L. Clough, *Radiat. Phys. Chem.*, **18**, 679 (1981).
8. M. V. Belousova, V. D. Skirda, O. E. Zgadzai, A. I. Maklakov, I. V. Potapova, B. S. Romanov, and D. D. Romyanthev, *Acta Polym.*, **36**, 557 (1985).
9. P. Dole and J. Chauchard, *Polym. Degrad. Stabil.*, **47**, 449 (1995).
10. P. Dole and J. Chauchard, *J. Appl. Polym. Sci.*, to appear.
11. K. T. Gillen, R. L. Clough, and J. Wise, *Polym. Preprints*, papers presented at the Chicago, IL, Meeting, Division of Polymer Chemistry Inc., American Chemical Society; p. 185.
12. G. Papet, L. Audouin-Jirackova, and J. Verdu, *Radiat. Phys. Chem.*, **33**, 329 (1989).
13. H. M. Le Huy, V. Bellenger, M. Paris, and J. Verdu, *Polym. Degrad. Stabil.*, **35**, 171 (1992).
14. S. Pauly, *Radiat. Phys. Chem.*, **39**, 269 (1992).
15. V. Langlois, L. Audouin, and J. Verdu, *Polym. Degrad. Stabil.*, **40**, 399 (1993).
16. H. Wilsky, *Radiat. Phys. Chem.*, **29**, 1 (1987).
17. H. Wilsky, *Radiat. Phys. Chem.*, **35**, 186 (1990).
18. K. T. Gillen, R. L. Clough, and C. A. Quintana, *Polym. Degrad. Stabil.*, **17**, 31 (1987).